

# Application of electrochemical techniques in investigation of the role of hydrogen in near-neutral pH stress corrosion cracking of pipelines

Y. F. Cheng · L. Niu

Received: 10 May 2006 / Accepted: 25 October 2006 / Published online: 20 January 2007  
© Springer Science+Business Media, LLC 2007

**Abstract** It has been acknowledged that hydrogen plays a critical role in near-neutral pH stress corrosion cracking (SCC) of pipelines. However, the accurate mechanism for hydrogen involvement remains unknown. This work reviewed the applications of various electrochemical techniques towards understanding near-neutral pH SCC. The techniques reviewed include electrochemical hydrogen permeation, cyclic voltammetry, electrochemical impedance spectroscopy, electrochemical noise and scanning photo-electrochemical microscopy. The manner by which these techniques allow for the investigation of the hydrogen evolution mechanism, adsorption/desorption and permeation kinetics and hydrogen diffusion and accumulation in steel as well as the interactions between hydrogen, anodic dissolution and stress at crack tip in near-neutral pH environmental condition is described. It is anticipated that the advanced electrochemical measurement techniques provide essential tools to investigate the mechanistic aspects on hydrogen involvement in near-neutral pH stress corrosion cracking in pipelines.

## Introduction

The study of hydrogen evolution reaction (HER) mechanism and adsorption/desorption kinetics has been paid considerable attention in the fields of electrochemistry, materials science, corrosion, surface science and energy storage [1–7]. In the corrosion area, knowledge of fundamental steps involved in hydrogen entry into the metals is of vital significance in protecting metals from undergoing hydrogen embrittlement (HE) or hydrogen-induced cracking (HIC) [1]. Proper characterization of the HER and hydrogen diffusion into metals requires the determination of the mechanism and kinetics of hydrogen evolution, hydrogen adsorption/desorption, hydrogen concentration and coverage on the surface, hydrogen absorption and diffusion through the metals, and defects and trapping effects as well as interactions between hydrogen, dissolution and applied stress [7–9].

Near-neutral pH stress corrosion cracking (SCC) on pipelines, cracking at pH of about 6.5, has been responsible for an increasing number of pipeline failures in recent years in Canada [10]. Previous work showed [11] that hydrogen could play an important role in near-neutral pH SCC in pipeline steels, altering the dissolution at and ahead of the crack-tip. The experimental results have indicated that the extracted soil solutions that result in more SCC susceptibility are always associated with higher hydrogen permeation current and sub-surface hydrogen concentration determined during electrochemical hydrogen permeation tests. Parkins [12] analyzed the potential-pH range where high pH SCC and near-neutral pH SCC occurred, and found that in the near-neutral pH solution, hydrogen discharge is possible. He concluded

---

Y. F. Cheng (✉)  
Department of Mechanical and Manufacturing Engineering,  
University of Calgary, Calgary, AB, Canada T2N 1N4  
e-mail: fcheng@ucalgary.ca

L. Niu  
School of Chemistry and Chemical Engineering, Shandong  
University, Jinan, Shandong 250100, China

that some synergistic effects between the hydrogen and the anodic dissolution exist during the growth of near-neutral pH SCC of pipelines.

There is a considerable amount of evidence [13–15] that hydrogen is involved in the near-neutral pH SCC of pipelines. However, the precise mechanism has not been identified. Recently, several models have been developed to determine the role of hydrogen in pipeline SCC. Gu et al. [16] deduced an equation for the synergistic effect of hydrogen and stress on the anodic dissolution rate. They suggested a local acidification generating during anodic dissolution, and thus thought that near-neutral pH SCC is dominated by the mechanism of hydrogen-facilitated dissolution. However, there is no further evidence to support this theory. With the underlying premise that the interaction between hydrogen and stress at the crack tip will increase the activation energy for anodic dissolution, Mao and Li [17] proposed a thermodynamic model to explain the interaction between the hydrogen and the stress at the crack-tip. In this model, they attributed the cathodic reaction to the reduction of hydrogen ions only, and ignored the reduction of water as the main cathodic process in deoxygenated, near-neutral pH solution. Furthermore, they did not take into account the effect of applied stress and the presence of cracks on the concentration of hydrogen atoms diffusing in the steels, and thus, over-simplified the thermodynamic consideration.

Cheng [9] developed a mechanistic model illustrating the interactions between hydrogen, anodic dissolution and stress at a crack tip by comprehensively considering the electrochemical reactions occurring on the line pipe steel in deoxygenated, near-neutral pH solution and by analyzing the changes of free-energy of the steel. According to the model, the hydrogen involvement depends on four factors: the effect of hydrogen on the anodic dissolution rate in the absence of stress, the effect of stress on the anodic dissolution rate in the absence of hydrogen, the synergistic effect of hydrogen and stress on the anodic dissolution rate at crack-tip and the effect of the variation of hydrogen concentration on the anodic dissolution rate. Development of the advanced electrochemical techniques such as scanning photo-electrochemical microscopy (SPEM) will enable the determination of these factors that are essential to understand the mechanistic aspects on the role of hydrogen in pipeline SCC.

This work reviews the application of the various electrochemical techniques in the investigation of the HER mechanism, adsorption/desorption kinetics, hydrogen permeation and diffusion in the steel, and the accumulation at crack tip to contribute to the

cracking process. The techniques reviewed include electrochemical hydrogen permeation, cyclic voltammetry (CV), electrochemical impedance spectroscopy (EIS), electrochemical noise (EN) and SPEM. Although the review focuses on the near-neutral pH SCC of pipelines, the various electrochemical techniques are applicable for hydrogen studies in other areas.

### Electrochemical hydrogen permeation technique

The electrochemical hydrogen permeation technique was developed by Devanathan and Stachurski in the 1960s to study the diffusion of hydrogen in metals [18–20]. In this technique, the metallic specimen is placed between two glass cells, one used for charging the specimen with hydrogen and the other for measuring the hydrogen flux permeating through the membrane, as shown in Fig. 1. The hydrogen flux through metals with time can be accurately determined since the small current resulting from oxidation of hydrogen at the exit surface of the membrane can be very accurately measured. The method is simple and very useful for the study of hydrogen absorption into different metals, alloys and coatings in the presence or absence of additives to the aqueous solution. The additives are added either to simulate the practical reactions in near-neutral pH environment [11–13], or to enhance the sensitivity of the technique [11]. It has also been used to study the trapping effect and hydrogen-defect interactions. To date, the electrochemical

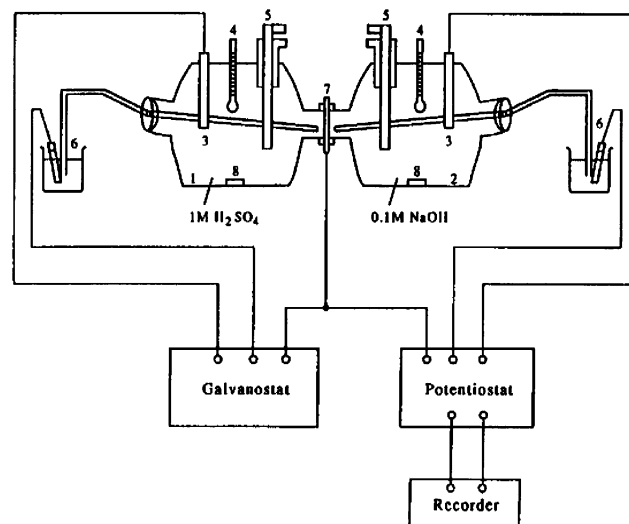


**Fig. 1** Schematic diagram of experimental apparatus: (1) permeation cell; (2) determination cell; (3) counter electrode; (4) thermocouple; (5) gas dispersion tube; (6) reference electrode with a Luggin capillary; (7) specimen; and (8) magnetic bar [20]

method of hydrogen permeation through metal membrane has been an important technique for the study of the diffusion and absorption of hydrogen in metals [21–25].

Generally, it is assumed that diffusion of hydrogen in the membrane is the slowest step in the overall hydrogen permeation process. However, hydrogen may be trapped at microstructural defects such as dislocations, grain boundaries, non-metallic inclusions, and other internal interfaces. Quantitative information, such as the hydrogen diffusion coefficient, sub-surface hydrogen concentration, coverage of the entrance side, the steady-state permeation rate and trapping of hydrogen [11, 26–28], can be obtained from the hydrogen permeation curves.

The electrochemical hydrogen permeation technique has been one of the main methods to investigate the hydrogen involvement in near-neutral pH SCC of pipelines. Cheng et al. [11] measured the permeation curves of hydrogen through X65 pipe steel in the various soil solutions extracted in Alberta and North Ontario, where SCC occurrences were recorded. By fitting the permeation current with the constant concentration model, they determined the hydrogen diffusion coefficients and sub-surface hydrogen concentrations. It is shown that there was little difference of hydrogen diffusivity through the metal in these solutions. However, the soil solution generating a higher sub-surface hydrogen concentration is associated with a higher susceptibility of the steel to SCC. Yan and Weng [29] used a monocell to investigate the absorbed hydrogen concentration in hydrogen pre-charged pipeline steels (X70 and 16Mn steels). The monocell was used for pre-charging hydrogen. On completion of hydrogen-charging, the specimen was immediately rinsed and transferred to another cell for hydrogen permeation current measurements. This method is different from the conventional double-cell method where hydrogen-charging and permeation current measurement were performed simultaneously. The advantage of using the monocell claimed by authors [29] was that it is easily to be used in field to measure and analyze hydrogen permeation. It was shown that the hydrogen oxidation current and hydrogen concentration in pre-charged 16 Mn steel were marginally higher than those in X70 steel, indicating that the former was more susceptible to hydrogen absorption than the latter. King et al. [30] performed the hydrogen permeation experiments using planar and hollow cylindrical samples of X56 and X70 pipeline steels in NS4 solution equilibrated with  $\text{CO}_2/\text{N}_2$  atmospheres. The work found that the hydrogen permeation depended on the potential of the steel, the surface

condition of the sample, and the applied stress. The influences of cathodic potential on the hydrogen content of a pipeline steel exposed to NS4 solution were also confirmed by He et al. [31]. Torres-Islas et al. [32] studied the effects of hydrogen on the mechanical properties of X70 pipeline steel at different heat treatment conditions by slow strain rate testing technique and electrochemical hydrogen permeation measurements. Hydrogen permeation increased with solution concentration and was maximum for the quenched steel. Pre-charging of specimens with hydrogen did not have any effect on the mechanical properties of the as-received or water-sprayed steel but it did in the quenched and the quenched + tempered steels. Thus, the microstructures of the steel generated during quenched treatment are sensitive to hydrogen effect. Contreras et al. [33] studied the susceptibility to SCC of the X52 and X70 pipeline steels using slow strain rate tests and hydrogen permeation measurements. It is found that corrosion was an important factor in the initiation of some cracks. The diffusion of atomic hydrogen was related to the fracture forms, and the hydrogen permeation flux increased with increasing temperature.

It has to be realized that the application of electrochemical hydrogen permeation test has some certain limits to obtain reproducible results [4, 6]. First, an appropriate specimen thickness is critical to this test. The upper limit for the thickness is controlled by the time to attain a steady-state condition for hydrogen permeation. If the specimen membrane is too thick, the time to perform an experiment will be impractically long, which will introduce other problems such as adsorption of impurities at the entry surface, and change in concentration (especially pH) of the electrolyte. Conversely, if the membrane is too thin, the rate-limiting step of the hydrogen permeation may be a surface reaction rather than the diffusion of hydrogen through the membrane. Furthermore, grain boundary effects become dominant in the thin membrane. Therefore, the lower limit of the specimen thickness should be at least five to ten times the average grain diameter [6]. Second, the surface of the specimen should be flat, well polished and free of film. If film exists on the entry side, some of the hydrogen-charging current will be spent to reduce it, resulting in a lower apparent hydrogen diffusion coefficient than the actual value. Third, a thin layer of palladium (Pd) is usually plated onto the anodic side of the specimen to protect the metal from dissolution. Finally, all impurities in the solution have to be removed to the lowest possible level to eliminate their adsorption on the specimen surface.

Furthermore, the hydrogen absorption and permeation into the steel during cathodic polarization depends on a number of factors including the composition of the steel, the solution pH, the level of cathodic polarization and the formation of a surface film [8]. It becomes difficult to obtain an accurate evaluation of the risk of hydrogen-induced degradation of the steel. For underground pipelines, the problem becomes even more complex because of the heterogeneous environments involved.

### Cyclic voltammetry

The CV technique establishes the different anodic and cathodic current–potential relations as a function of various environmental conditions [34]. In CV measurements, the cathodic/anodic polarization current is monitored while the potential applied on the specimen is swept from the pre-set lower limit to the upper limit, and then back to the lower limit. The potential sweep could be performed by a few cycles at the various sweep rates. The characteristic electrode reactions occurred at the specific potential are indicated by the recorded current peaks or potential shoulders. The polarization behavior of the electrode will be studied by analyzing the cyclic voltammograms. Thus, as an effective method to study the electrode process kinetics, CV measurements provide mechanistic information such as electrode reaction, adsorption/desorption process, intermediate species, surface coverage, rate-controlling step, etc. Moreover, the CV technique enables the investigation of the fundamental aspects associated with HER mechanism and kinetics at the metal/electrolyte interface and hydrogen adsorption/desorption process as well as the hydrogen absorption and entry into the metal.

Gabrielli et al. [35] used the CV technique to study the hydrogen absorption on Pd thin film (10 monolayers and 100  $\mu\text{m}$ ). It was demonstrated that the absorption of hydrogen into the Pd thin layer prepared by electrodeposition is different from that of the bulk Pd. On the thin Pd film, hydrogen adsorption, absorption and evolution processes are separated. Moreover, the adsorption kinetics depends strongly on layer thickness.

Flis et al. [36] investigated the hydrogen entry into iron at low anodic and low cathodic polarizations in neutral and alkaline solutions, and found that, with the conjunction of CV with electrochemical hydrogen permeation technique, the peaks of hydrogen permeation rate existed for iron at a low anodic polarization potential during positive potential sweeps, and at

slightly more negative potentials in the reverse sweeps. It is concluded that CV can be used for a quick survey of the potential dependence of hydrogen entry in iron and steel in a variety of electrochemical conditions.

Parkins et al. [37] used the potentiodynamic and galvanostatic polarization techniques to investigate the relationship between potential and current density for a pipeline steel in carbonate–bicarbonate solution as a function of temperature and solution composition. It is concluded that the reasons for pipeline surfaces maintaining specific potentials when subjected to cathodic currents were recognizable in terms of reactions between the constituents of mill-scaled surfaces and the environments with which they were likely to be in contact if the conditions for SCC were to be met. The presence of  $\text{Fe}_3\text{O}_4$ , a major constituent of mill scale, on the surface could promote potentials within the range where SCC was possible, under galvanostatic conditions simulating the application of cathodic protection to a pipeline.

To develop a mechanistic understanding of the polarization behavior of pipeline steel in near-neutral pH solution, King et al. [30] used the CV technique to study the voltammetric behavior of X-56 pipeline steel in deoxygenated N1 trapped water. As shown in Fig. 2, the extent of catalysis of the HER is dependent upon the potential to which the electrode is scanned during the prior oxidation cycle, i.e., to the extent of oxidation of the surface. If the surface is only oxidized as far as Peak I, the HER current on the reverse scan is slightly higher than that during the forward scan on the reduced surface; If, however, the surface is scanned as far as Peak II (corresponding to the formation of  $\text{Fe}(\text{OH})_2$ ), the rate of hydrogen reduction on the

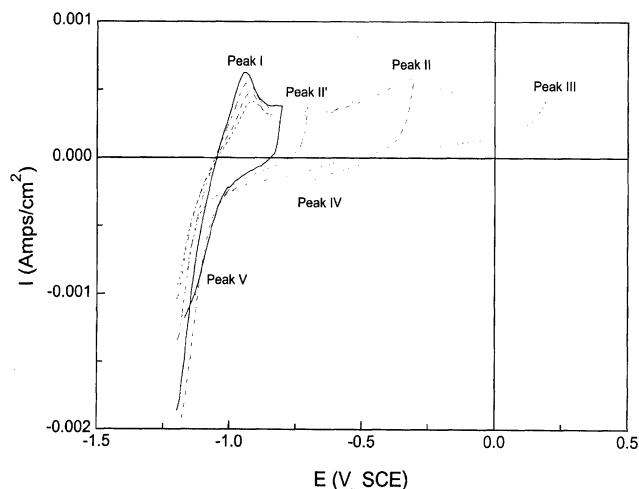


**Fig. 2** Cyclic voltammogram of X-56 steel in anaerobic N1 trapped water (pH 9.5 at 25 °C). Scan rate 100  $\text{mV s}^{-1}$  [30]

reverse scan is an order of magnitude or more higher than on the forward scan. The higher current on the reverse scan is not due to the reduction of an oxide layer formed during the forward scan because the charge passed during the reverse scan far exceeds that associated with Faraday processes during the forward scan. This catalysis of the HER is believed to be due to the simultaneous presence on the surface of Fe sites in more than one oxidation state (either Fe(0) and Fe(II) or Fe(I) and Fe(II)). Rapid electron exchange is facilitated by redox reactions between the surface sites and the result is more rapid hydrogen evolution than on surfaces entirely covered by surface sites of the same valence (e.g., fully reduced Fe(0) or fully oxidized Fe(II) surfaces). Thus, when the surface is fully oxidized (i.e., when the potential is scanned to Peak III), the subsequent rate of the HER on the reverse scan is lower than when the potential was scanned into Peak II. Similarly, once the surface is reduced as the potential is scanned negatively, the surface catalytic behavior is lost, and a sharp “peak” (Peak V) is observed in the HER region.

### Electrochemical impedance spectroscopy

EIS provides a non-destructive, effective technique for studying the mechanisms and kinetics of the interfacial electrochemical reaction. In EIS measurements, broad range of the applied frequency allows for the investigation of reactions occurring over a wide range of kinetics, such as the corrosion electrochemistry of the coated steel, since it distinguishes between the many phenomena that contribute to the charge-transfer rate. Furthermore, the Kramers–Kronig (K–K) transforms have been used to ensure the experimental data validity. However, the interpretation of the impedance data is relatively difficult. The impedance for many practical systems such as well-inhibited solutions, polymer-coated metals, and anodized aluminum do not reach a stable DC limit in the frequency range which is experimentally accessible. EIS can be measured and analyzed to characterize the hydrogen evolution and adsorption/desorption processes at the metal/electrolyte interface as well as the hydrogen absorption and diffusion in the metal.

Pyun and co-workers [38–40] characterized the hydrogen absorption and diffusion into the Pd membrane by EIS. Authors simulated the complex-plane impedance spectra and the steady-state current density vs. overpotential curve in terms of the kinetic rate constants of Volmer adsorption, hydrogen absorption

reaction and the hydrogen diffusivity in palladium, and theoretically calculated the steady-state hydrogen coverage as a function of overpotential. At the overpotentials below 0.08 V (SHE), the steady-state hydrogen coverage showed higher values than the atomic ratio of H/Pd of 0.03 (maximum solubility of  $\alpha$ -phase palladium), indicating the formation of  $\beta$ -palladium hydride. It is suggested that the direct hydrogen absorption without passing through the adsorbed phase, accompanied by the anomalous hydrogen permeation, accounts for the formation of  $\beta$ -phase palladium hydride in the interfacial region of palladium membrane electrode as a thin layer at the overpotentials lower than 0.08 V (SHE). The authors found a transition potential dominating the indirect and direct hydrogen absorption reaction. Moreover, the formation of palladium hydride, indicated by the EIS plot, acted as a barrier for hydrogen diffusion in the electrode.

As a successive work to study the hydrogen adsorption and absorption in Pd thin films, Gabrielli et al. [41] measured EIS of Pd films with various thicknesses, deposited on a gold electrode, in the potential range where hydrogen absorbs in Pd. One of the main results was the observation of a maximum charge-transfer resistance ( $R_{ct}$ ) as a function of electrode potential. The maximum  $R_{ct}$  decreased with the increasing film thickness. This behavior was attributed to the trapping of the hydrogen atoms in a sublayer just under the electrode surface and a direct exchange of the trapped hydrogen with the electrolyte.

Bruzzoni et al. [42] studied the hydrogen diffusion in  $\alpha$ -iron by electrochemical hydrogen permeation and EIS to define a new transfer function for hydrogen permeation through metallic membranes. The determination of the permeation transfer function revealed information about the electrochemical mechanisms of hydrogen discharge on the metallic surface, such as, a theoretical model developed to obtain an analytical expression of the permeation transfer function, a value of  $9.6 (\pm 0.6) \times 10^{-9} \text{ m}^2/\text{s}$  for the hydrogen diffusion coefficient through iron at 25 °C that is independently of both the membrane thickness and the hydrogen-charging solution pH, and the potential range that can be applied, both at the input and output surfaces, to maintain validity of the theoretical model for 0.1 M NaOH solution: cathodic charging potential  $E_c \leq -1.75 \text{ V}$  and the anodic detection potential  $-0.2 \text{ V} > E_d > -0.5 \text{ V}$ .

EIS technique has been used to detect localized corrosion including SCC. Bosch [43], with systematic considerations of anodic dissolution, hydrogen evolution and water reduction under different conditions,

developed an impedance model showing a phase shift of the impedance at particular frequencies that were related to a stress corrosion crack. Theoretical calculation showed that there was an optimum test frequency for each crack length.

### Electrochemical noise

EN is the spontaneous fluctuations of corrosion current and/or potential generated by corrosion reactions [44, 45]. The EN technique has unparalleled advantages to study the corrosion phenomena with a random nature. In EN measurements, a pair of nominally identical metal working electrodes (WE) and a reference electrode (RE) is connected with a zero-resistance ammeter. The galvanic current flowing between the two WEs and the potential difference between the coupled WEs and the RE are measured as the current and potential noise. With electrodes under potentiostatic control, a conventional three-electrode electrochemical cell is used for current transient measurements [46–49]. The time and frequency processing techniques devised for random signals can be applied for EN data. In the case where the elementary noise transients are not too numerous and are discernable, a statistical counting can be done on the time series to evaluate a mean appearance rate [49–51]. However, in the case where many events occur at the same time and their transients overlap, a spectral analysis of the random signal in the frequency domain will allow the characteristic parameters of the process to be attained [52].

For V-profile weld joints where the difference in chemical composition and microstructure across the thickness of the sample precludes the preparation of thin membranes or even small electrodes that could represent the bulk characteristic of those materials, it is almost impossible to prepare this kind of sample for direct hydrogen permeation measurements. Silva et al. [53] investigated the possibility of gathering indirect information about atomic hydrogen absorption into standard cylindrical electrodes in a single-compartment cell from the EN generated by hydrogen bubble evolution. It is a preliminary attempt to employ the EN technique on hydrogen evolving electrodes as an alternative tool to detect and quantify atomic hydrogen absorption in practical situations where the use of specific cells and samples is precluded. It was shown that electrolyte resistance fluctuations provided better reliability to the estimation of the bubble evolution characteristic parameters (detachment size and rate)

than potential fluctuations, and were related to the intrinsic behavior of Pt and Pd electrodes concerning atomic hydrogen absorption. Authors used the spectral analysis method to derive the expression of power spectral density (PSD) of the potential fluctuations relating the hydrogen evolution characteristic parameters such as the bubble detachment mean radius, the bubble detachment mean rate, and the mean volume of hydrogen released under gas form per time unit. These parameters were directly derived from the electrolyte resistance fluctuations generated by hydrogen evolution, which were measured simultaneously with the potential fluctuations. The PSD calculated at the different current densities in the frequency domain were then determined, as shown in Fig. 3. It is seen that EN results were in good agreement with those obtained by direct measurements of absorption flux as reported in the literature, indicating that this kind of approach may be an alternative tool to investigate hydrogen absorption susceptibility.

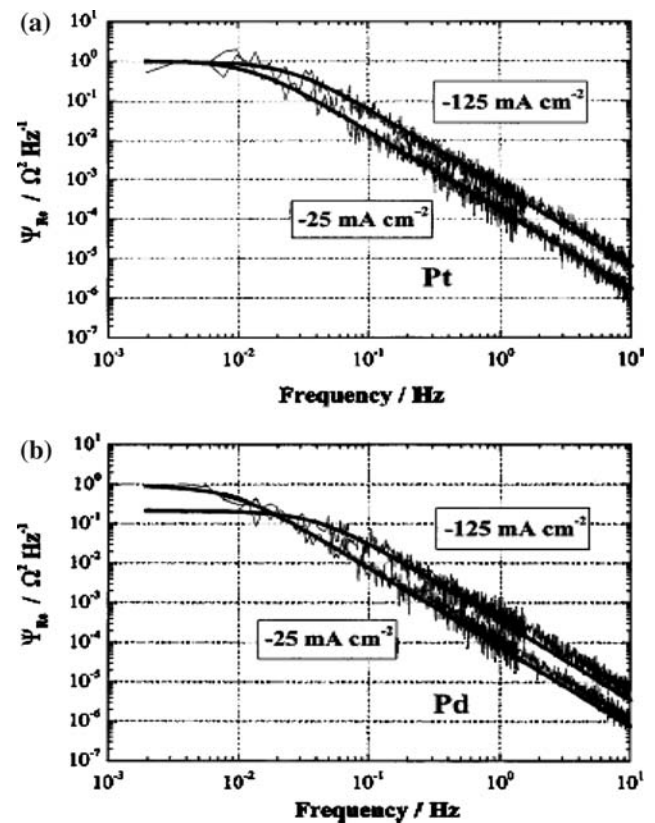


**Fig. 3** Measured and simulated noise spectra for 0.2 cm<sup>2</sup> stationary Pt (a) and Pd (b) electrode at current densities of –25 and –125 mA/cm<sup>2</sup> [45]

## Scanning photo-electrochemical microscopy

It is acknowledged [54–56] that the photo-electrochemical studies of passive film could provide valuable information about the film composition and structure and the mechanism of electrochemical processes occurring during corrosion. Moreover, photo-electrochemical imaging has been suggested as a good tool to map out the defects, the spatial variation of composition, and the microstructure of passive films [57, 58]. To both dynamically and directly monitor the emerging consequences of hydrogen permeation flux in terms of microstructural characteristics, a technique named SPEM was developed in 1993 [59].

SPEM is a technique able to visualize in situ and in real-time the hydrogen distribution in the steel with a spatial resolution of about 10  $\mu\text{m}$ . The hydrogen concentration is proportional to the measured photo-current response. Figure 4 shows the schematic diagram of SPEM [60]. The basic principle of SPEM is based on the improved photo-response owing to the photo-oxidation of hydrogen atoms when a passivated steel is loaded with hydrogen and illuminated. During scanning the steel specimen by a laser spot, a well-detailed image of hydrogen in the steel will be obtained. The main configuration features include a

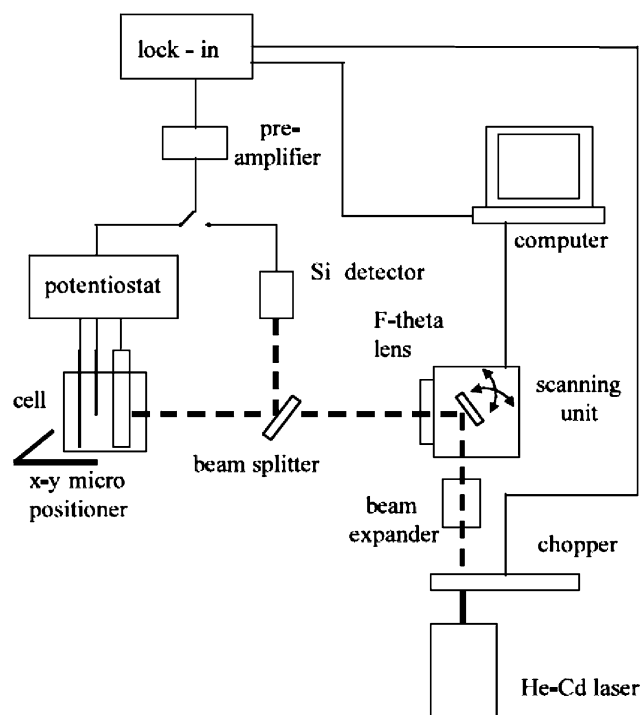


**Fig. 4** Experimental set-up of scanning photo-electrochemical microscopy technique [60]

25 mW argon ion laser source with wavelength of 488–515 nm to emit light beam, a chopper to chop the light at 60 Hz, a frame grabber to control the rotation of mirrors in slow scan mode, an electrochemical cell with quartz window to hold working electrode, reference and counter electrodes, an electrochemical system to record photo-current, a pre-amplifier and a lock-in amplifier to amplify the photo-signals, and a computer system to record and display the image. The magnification of the image is modified by varying the scanning area size. Thus, SPEM maps the distribution and concentration of hydrogen in sites such as crack tip, grain boundaries, corrosion pits, inclusions and other defects, and provides essential data to evaluate the influence of hydrogen on the initiation and growth of cracks.

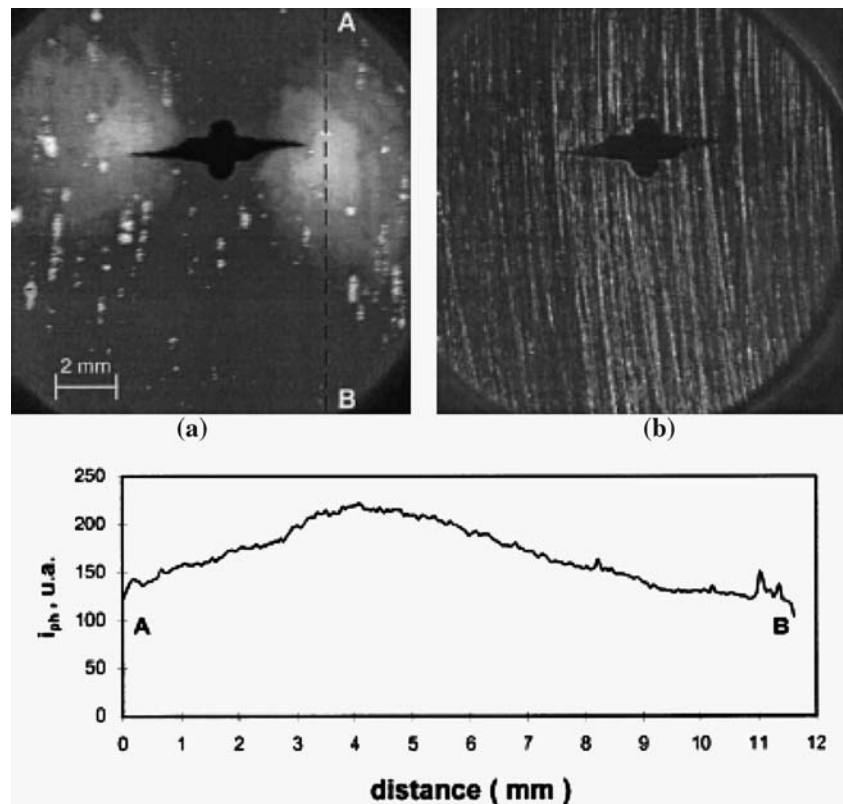
The SPEM image of the region ahead of the crack tip in an unloaded X60 pipe steel specimen after hydrogen-charging is shown in Fig. 5 [61]. It provides image of the local distribution of hydrogen in high stress field regions, where the plastic structure segregates large amounts of hydrogen. The resulting images do not provide the actual concentration of hydrogen atoms in the lattice because the laser beam at the surface is able to detect only the mobile and not the trapped atoms. This fact is particularly relevant in the metal regions where the structure is stressed and the concentration of the dislocations, which trap large amounts of hydrogen atoms, is enhanced.

Hydrogen permeation through a welded joint of A516-60 steel immersed in a  $\text{H}_2\text{S}$  solution was investigated using the SPEM [62]. The photoimages show that, at the same backup scale, the photoresponse is irreversibly affected by hydrogen flux. It is observed a delay in the photocurrent response of the welded region related to the base metal and adjoining regions. This behavior indicates that a higher solubility of hydrogen at the welded region in the metal lattice than the other regions. The investigation demonstrated that the SPEM technique as an useful tool to monitor with an optical probe in real time, in situ and under continuous hydrogen charging the different hydrogen diffusivity in areas with different hydrogen solubility and different microstructure of metals susceptible to hydrogen permeation and coated by an oxide film with semiconducting properties.

## Other techniques

In addition to the electrochemical techniques mentioned above, there are some other chemical and

**Fig. 5** (a) SPEM image of the region ahead of the crack tip in an unloaded X60 steel specimen after hydrogen charging. (b) Optical image of the same region obtained by the reflected laser beam which scans the steel surface. (c) Photo-current profile along the A–B line in the SPEM image [61]



surface physical techniques to investigate the hydrogen in the metals.

#### Thermal desorption spectroscopy (TDS) [63, 64]

In TDS method, the hydrogen effusion is measured in dependence on temperature at constant heating rates and sample thickness. Generally, one or multiple desorption peaks could be detected by TDS, which reflect the hydrogen effusion from a main binding state or the multiple trapping sites. The technique is most advantageous when applied to materials with a low hydrogen diffusion coefficient. This method can be used in conjunction with electrochemical hydrogen permeation technique to investigate the hydrogen diffusion, solubility and trapping behavior in metals.

#### Secondary ion mass spectroscopy (SIMS) [17]

SIMS is a surface analytical technique used for obtaining elemental and molecular chemical information on surfaces (static SIMS), and for detecting ppb-level concentration of impurities in semiconductors and metals (dynamic SIMS). All elements, including hydrogen, are detectable by SIMS. In SIMS analysis, the sample is placed in an ultrahigh vacuum environment where the primary ions bombard and sputter

atoms, molecules and molecular fragments from the sample surface. The mass of the ejected particles, i.e., secondary ions, is analyzed via time-of-flight mass spectrometry.

#### Gas chromatography (GC) [65]

GC method has been developed for assessing the level of hydrogen in metals by means of first releasing the hydrogen from metal samples by heat or vacuum fusion, and then measuring the amount released using a gas chromatograph. Different from TDS, the GC method discerns the overall hydrogen amount and cannot locate the trapping states.

#### Ion beam [66]

The ion-beam experiment provides a substantial body of previously unavailable information and yields new mechanistic understanding and broad capabilities for quantitative prediction. A representative experiment performed by authors [67] began with the room temperature implantation of 15 keV  $^4\text{He}^+$  ions and 750 keV  $^3\text{He}^+$  ions into well-annealed iron, the respective fluences being  $4 \times 10^{16}$   $^4\text{He}^+$  ions  $\text{cm}^{-2}$  and  $4 \times 10^{16}$   $^3\text{He}^+$  ions  $\text{cm}^{-2}$ . After helium implantation the specimen was cooled to about 120 K and implanted



with  $1 \times 10^{16}$  D<sup>+</sup> ions cm<sup>-2</sup> at 15 keV. The theoretically calculated depth profiles resulting from the implantations will be obtained. The interaction between hydrogen and other entities within the metal matrix seems to be one of the most critical questions for near-neutral pH SCC. Ion-beam studies elucidate hydrogen trapping by vacancies, vacancy-solute complexes, helium bubbles and crystalline precipitates and characterize the phase-change reactions involving hydride precipitation, hydrogen-bubble formation and hydrogen reduction of oxides.

### Acoustic emission (AE) [67]

AE technology is a nondestructive testing method that has a high sensitivity for detecting active microscopic events such as plastic deformation, cracking and phase transformation, within a material. These events give rise to elastic waves which propagate out into the material and result in detectable AE signals. Nowadays, the study is aimed to investigate the characteristics of the AE signals resulting from hydrogen permeation processes into the metals. Weng et al. [67] investigated the characteristics of AE signals detected from the hydrogen permeation test of a medium strength steel. The test results showed that the more severe the hydrogen damage, the higher was the AE energy that could be detected. In addition, the variations in the detected AE signals were found to have a close correlation with the variations in the hydrogen permeation current. With increasing hydrogen permeation current, both the accumulated AE energy and the AE events were found to increase accordingly. For the specimens subjected to hydrogen-induced blistering, the detected AE energy level and the amplitude distribution pattern were found to be different from those detected from the specimen without blistering. This observation may contain potential information for distinguishing between the severity of hydrogen-induced damage.

### Conclusions

Hydrogen evolution and entry into the steel play a critical role in near-neutral pH SCC of pipelines. The various electrochemical techniques could provide mechanistic information about the hydrogen involvement.

The electrochemical hydrogen permeation technique has proved to be very useful in studies of the hydrogen entry in metals because of its simplicity, high sensitivity, and flexibility with regard to experimental

conditions. CV, EIS and EN techniques provide powerful tools to characterize the surface and interface reactions during the processes of hydrogen evolution, adsorption/desorption on metals surface, and absorption in metals.

Scanning photo-electrochemical microscopy enables visualization in situ and in real-time of the hydrogen distribution and concentration in the steel, and thus, provides an ideal tool to understand the role of hydrogen in the initiation and propagation of stress corrosion cracks.

**Acknowledgements** This work was supported by Canada Research Chairs program and Natural Science and Engineering Research Council of Canada (NSERC).

### References

- Smialowski M (1977) In: Staehle RW (ed) Stress corrosion cracking and hydrogen embrittlement of iron based alloys. NACE, Houston, p 405
- Mccright RD (1977) In: Staehle RW (ed) Stress corrosion cracking and hydrogen embrittlement of iron based alloys. NACE, Houston, p 306
- Oriani RA, Hirth JP, Smialowski M (1985) In: Hirth JP, Oriani RA, Smialowski M (eds) Hydrogen degradation of ferrous alloys. Noyes Publications, Park Ridge, NJ, p 101
- Deluccia JJ (1988) In: Raymond L (ed) Hydrogen embrittlement: prevention and control. ASTM, Philadelphia, PA, p 17
- Ohnaka N, Furutani Y (1990) Corrosion 46:129
- Iyer RN, Pickering HW (1990) Ann Rev Mater Sci 20:299
- Cheng YF, Du YL (1993) Corrosion 53:776
- Ovshinsky SR, Fetcenko MA, Venkatesan S, Chao B (1995) In: Conway BE, Jerkiewicz G (eds) Electrochemistry and materials science of cathodic hydrogen absorption and adsorption. The Electrochemical Society Proceedings Series, PV 94-21, Pennington, NJ, p 344
- Cheng YF (2006) J Mater Sci, DOI: [10.1007/s10853-006-1375-y](https://doi.org/10.1007/s10853-006-1375-y)
- National Energy Board (1996) In: Report of public inquiry concerning stress corrosion cracking on Canadian oil and gas pipelines. MH-2-95, p 7
- Cheng YF, Yang L, King F (2000) In: Proceedings of the international pipeline conference. ASME, Calgary, p 1479
- Parkins RN (2000) In: Corrosion'2000, paper no. 363. NACE, Houston
- King F, Jack TR, Chen W, Wang SH, Elboudjaini M, Revie W, Worthingham R, Dusek P (2001) In: Corrosion'2001, paper no. 1214. NACE, Houston
- Parkins RN, Delanty BS (1996) In: Proceedings of the ninth symposium on pipeline research, catalogue no. L51746. PRCI, p 19-1
- Plumtree A, Lambert SB, Sutherby R (1996) In: Corrosion-deformation interactions CDI'96, European Federation of Corrosion Publications. The Institute of Materials Research, Nice, France, p 263
- Gu B, Luo JL, Mao X (1999) Corrosion 55:96
- Mao SX, Li M (1998) J Mech Phys Solids 46:1125
- Devanathan MAV, Stachurski Z (1962) Proc Roy Soc A270:90

19. Devanathan MAV, Stachurski Z, Beck W (1963) *J Electrochem Soc* 110:886
20. Devanathan MAV, Stachurski Z (1964) *J Electrochem Soc* 111:619
21. Zakroczymski T (2006) *Electrochim Acta* 51:2261
22. Weng CC, Lin GC, Chen RT (1992) *Mater Sci Eng* 154:51
23. Ng HC, Newman RC (2005) *Corros Sci* 47:1197
24. Kurkela M, Latanision RM (1981) *Scripta Metall* 15:1157
25. Zhang TY, Zheng YP (1998) *Acta Mater* 46:5023
26. Bockris JOM, Breen JMC, Nanis L (1965) *J Electrochem Soc* 112:1025
27. Turnbull A, Saenz De Santa Maria M, Thomas ND (1989) *Corros Sci* 29:89
28. Kato C, Grabke HJ, Egert B, Pantzner G (1984) *Corros Sci* 24:591
29. Yan M, Weng Y (2006) *Corros Sci* 48:432
30. King F, Chen W, Wilmott M, Fessler RR, Krist K (2000) In: *Corrosion'2000*, paper no. 00361. NACE, Houston
31. He D, Chen W, Luo JL (2004) *Corrosion* 60:778
32. Torres-Islas A, Salinas-Bravo VM, Albarran JL, Gonzalez-Rodriguez JG (2005) *Int J Hydrogen Energy* 30:1317
33. Contreras A, Albiter A, Salazar M, Perez R (2005) *Mater Sci Eng A* 407:45
34. Bard AJ, Faulkner LR (2000) *Electrochemical methods: fundamentals and applications*, 2nd edn. John Wiley & Sons, New York, p 154
35. Gabrielli C, Grand PP, Lasia A, Perrota H (2004) *J Electrochem Soc* 151:1937
36. Flis J, Zakroczymski T (1992) *Corrosion* 48:530
37. Parkins RN, O'dell CS, Fessler RR (1984) *Corros Sci* 24:343
38. Lim C, Pyun SI (1993) *Electrochim Acta* 38:2645
39. Lim C, Pyun SI (1994) *Electrochim Acta* 39:363
40. Yang TH, Pyun SI (1996) *Electrochim Acta* 41:843
41. Gabrielli C, Grand PP, Lasia A, Perrota H (2004) *J Electrochem Soc* 151:1943
42. Bruzzoni P, Carranza RM, Collet Lacoste JR, Crespo EA (1999) *Electrochim Acta* 44:2693
43. Bosch RW (2005) *Corros Sci* 47:125
44. Dawson JL (1996) In: Kearns JR, Scully JR (eds) *Electrochemical noise measurement for corrosion applications*. ASTM STP 1277, West Conshohocken, PA, p 3
45. Eden DA, Rothwell AN (1992) In: *Corrosion'1992*, paper no. 292. NACE, Houston
46. Cheng YF, Rairdan B, Luo JL (1998) *J Appl Electrochem* 28:1371
47. Cheng YF, Wilmott M, Luo JL (1999) *Corros Sci* 41:1245
48. Cheng YF, Wilmott M, Luo JL (1999) *Appl Surf Sci* 152:161
49. Cheng YF, Luo JL (1999) *J Electrochem Soc* 146:970
50. Cheng YF, Wilmott M, Luo JL (1999) *Br Corros J* 34:280
51. Cheng YF, Luo JL (2000) *Br Corros J* 35:125
52. Cheng YF, Wilmott M, Luo JL (2000) *Electrochim Acta* 45:1763
53. Silva JM, Nogueira RP, De Miranda L, Huetb F (2001) *J Electrochem Soc* 148:E241
54. Cheng YF, Luo JL (1999) *Electrochim Acta* 44:2947
55. Cheng YF, Luo JL (2000) *Appl Surf Sci* 167:113
56. Stimming U (1986) *Electrochim Acta* 31:415
57. Kozłowski MR, Tyler PS, Smyrl WH, Atanasoski RT (1988) *Surf Sci* 194:505
58. Schmuki P, Bohni H (1994) *J Electrochem Soc* 141:362
59. Razzini G, Peraldo Bicelli L, Scrosati B (1993) *Electrochim Acta* 38:89
60. Maffi S, Lenardi C, Bozzini B, Bicelli LP (2002) *Measure Sci Technol* 13:1398
61. Razzini G, Cabrini M, Maffi S, Mussati G, Peraldo Bicelli L (1999) *Corros Sci* 41:203
62. Guedes FMF, Maffi S, Razzini G, Peraldo Bicelli L, Ponciano JAC (2003) *Corros Sci* 45:2129
63. Ningshen S, Uhlemann M, Schneider F, Khatak HS (2001) *Corros Sci* 43:2254
64. Von Zeppelin F, Haluška M, Hirscher M (2003) *Thermochim Acta* 404:251
65. Addach H, Berçot P, Wery M, Rezrazi M (2004) *J Chromatogr A* 1057:219
66. Myers SM, Wampler WR, Besenbacher F, Robinson SL, Moody NR (1985) *Mater Sci Eng* 69:397
67. Weng CC, Lin GC, Chen RT (1992) *Mat Sci Eng A* 154:51